NON-DUCTILE SEISMIC PERFORMANCE OF REINFORCED CONCRETE WALLS IN AUSTRALIA

Ryan Hoult[1,4], Helen Goldsworthy[2,4], Elisa Lumantarna[3,4]

ABSTRACT: *Much of the Australian building stock comprises of reinforced concrete (RC) buildings that rely on RC walls or cores as their lateral load resisting system. Past research on the seismic behaviour of RC walls has primarily concentrated on highly reinforced and confined sections. However, there is a paucity of research focusing on lightly reinforced and unconfined sections that are commonly found in regions of low to moderate seismicity such as Australia. Moreover, some lightly reinforced concrete walls have been observed to perform poorly in recent earthquake events, with a single crack forming at the base within the plastic hinge region in contrast to the expected distributed cracks. This paper reports on an investigation into the seismic performance of rectangular walls with typical detailing and design parameters found in Australia. A simple model that can be used to predict the required amount of longitudinal reinforcement for the onset of secondary cracking is introduced. Finite element modelling results emphasise that a minimum amount of longitudinal reinforcement is required for secondary cracking to occur. Ultimately this will be useful for deriving a plastic hinge length that can be used for displacement capacity calculations of lightly reinforced walls.*

KEYWORDS: Non-ductile, RC, walls, secondary cracking, plastic hinge, VecTor2

[1] Ryan Hoult, Department of Infrastructure Engineering, University of Melbourne. Email: rhoult@student.unimelb.edu.au
[2] Helen Goldsworthy, Department of Infrastructure Engineering, University of Melbourne. Email: helenmg@unimelb.edu.au
[3] Elisa Lumantarna, Department of Infrastructure Engineering, University of Melbourne. Email: elu@unimelb.edu.au
[4] Bushfire and Natural Hazards Cooperative Research Centre, Melbourne Australia

1 INTRODUCTION

The focus of this research is to demonstrate that a minimum longitudinal reinforcement ratio ($\rho_{wv.min}$) is needed to initiate secondary cracking in reinforced concrete (RC) walls. A simple secondary cracking model (SCM) is introduced that estimates the amount of steel reinforcement needed to allow secondary cracking when an RC section is subjected to large flexural actions. A finite element modelling program, VecTor2 [1], is then used to validate the SCM for a mid-rise (MR) RC wall with a range of longitudinal reinforcement ratios (ρ_{wv}). The RC wall has detailing and design parameters that are typically found in low-to-moderate seismic regions, such as Australia. An equivalent plastic hinge length (L_p) is calculated from the walls analysed in VecTor2. The results from the SCM and VecTor2 indicate a much higher ρ_{wv} is required to initiate secondary cracking in the concrete.

2 BACKGROUND

In regions of low-to-moderate seismicity, such as Australia, the majority of the RC walls are lightly reinforced [2, 3]. Poor performance associated with the seismic performance of lightly reinforced walls has been observed in recent earthquake events [4, 5]. Most notably, a single crack has been found to form in the plastic hinge zone of lightly reinforced walls leading to large strain concentrations in the reinforcement at this crack and potentially to fracture of the reinforcement. For instance, it was likely that the RC core wall of the Pyne Gould Corporation building, which collapse in a non-ductile, brittle and catastrophic fashion during the February 22nd 2011 Christchurch earthquake, had insufficient longitudinal reinforcement to transmit the required tension to initiate secondary cracking in the surrounding concrete [4]. Thus, in comparison to the expected distribution of cracks (and corresponding distribution of strains) up a significant portion of the wall height as is usually assumed when determining the plastic hinge length, the yielding of reinforcement was 'confined to a short length resulting in a single wide crack in the potential plastic region at level 1' [4]. Another lightly reinforced wall that was observed to have a single crack at the base after the Christchurch event, with fractured longitudinal reinforcement crossing the crack, was located in the Gallery Apartments Building [4]. Some studies confirmed that the wall had insufficient reinforcement to allow secondary cracking [6-8]. 'The building's overall damage state may be described as being at near collapse' [9].

3 SECONDARY CRACKING MODEL

Lightly reinforced walls will exhibit a single crack, and hence large strain concentrations in the longitudinal reinforcement crossing this crack, at the base of the wall when subjected to large lateral motions if the cracking moment (M_{cr}) is larger than the ultimate moment of the RC wall (M_u) [6, 10, 11]. The cracking moment capacity of an RC wall can be calculated using the fundamental bending stress equation and incorporating the stress due to axial load, given in Equation 1.

$$M_{cr} = \frac{\left(f'_{ct.f} + \frac{P}{A_g}\right) t L_w^2}{6} \quad (1)$$

where $f'_{ct.f}$ is the characteristic flexural tensile strength of concrete, P is the axial load, A_g is the gross section area, t is the thickness of the wall and L_w is the length of the wall.

In the Concrete Structures design standard of Australia, AS3600:2009 [12], the ultimate design strength in bending for RC beams must be larger than or equal to $1.2M_{cr}$ (Clause 8.1.6.1). Some authors [13] believe that this Clause in AS3600:2009 is also provisional for the design of slabs and walls in bending by implication, although this is not transparently indicated in the Standard.

Recent research has indicated that the brittle type of failure with a single crack forming in the plastic hinge region can still occur even if M_u is larger than M_{cr} [9]. For a distribution of cracks to form, the stress transmitted from the longitudinal reinforcing steel to the surrounding concrete (σ_{con}) must be larger than the flexural tensile strength of the concrete ($f'_{ct.fl}$). However, the axial stress (σ_A) could also be taken into consideration. If it is assumed that these stresses are equal, it is possible to calculate the necessary spacing (s) required between the longitudinal reinforcement and hence calculate the required minimum longitudinal reinforcement ratio ($\rho_{wv.min}$). In this case, the $f'_{ct.fl}$ is assumed to be equal to the upper characteristic value taken from the Model Code 2010 [14] of $0.396(f_{cmi})^{(2/3)}$, where f_{cmi} is the in situ compressive strength of concrete. Equations 2-4 are the simplified calculations for a SCM, which finds the $\rho_{wv.min}$. The SCM is dependent on the thickness of the wall (t), number of rows (n_t) and diameter (d_{bt}) of transverse (horizontal) steel reinforcement and the ultimate stress of the longitudinal steel reinforcement (f_u). Some of these parameters are also illustrated in Figure 3.1.

$$s = \frac{f_u}{t_{eff}(f'_{ct.fl} + \sigma_A)} \quad (2)$$

$$t_{eff} = t - n_t d_{bt} \quad (3)$$

$$\rho_{wv.min} = \frac{1}{s.t} \quad (4)$$

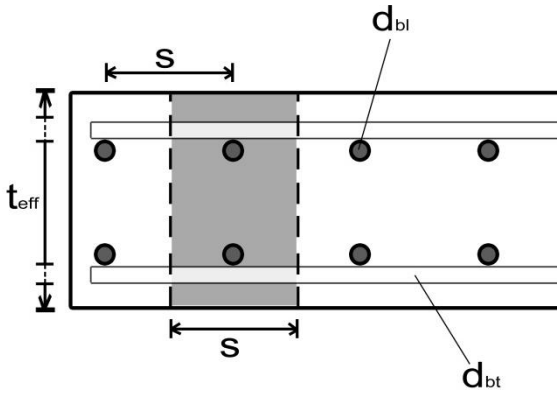

Figure 3.1: *Cross section of a typical RC rectangular wall*

Using Equations 2-3, the $\rho_{wv.min}$ required for secondary cracking can be calculated for a wall with typical values that would be representative of a low-to-moderate seismic region, such as Australia. A value of 60MPa for the f_{cmi} was used, which corresponds to a $f'_{ct.f}$ of 6.07MPa. This was assuming that typical values for the 28-day compressive strength of concrete (f'_c) used in the design of RC walls was around 32-40MPa, and the strength has increased due to the initial variability as well as the increase of strength with age. This was not an unreasonable assumption as, for example, the concrete strengths from the Pyne Gould and Gallery Apartments buildings were found to range from 1.86 to 2.4 times the initial f'_c value aimed for in design [15, 16]. A mean value for f_u of 660MPa [17] for Grade D500N steel reinforcement was used for the 12mm diameter bars. The wall was assumed to be 200mm thick with two layers of transverse and longitudinal reinforcement, one close to each face of the wall. Using the SCM calculations, the $\rho_{wv.min}$ using these parameters is equal to 0.81%. If an axial load ratio (ALR) of 5% (corresponding to an axial stress of 3MPa) is assumed to be subjected on the wall, the $\rho_{wv.min}$ is equal to 1.21%. This indicates that the SCM estimates a much higher minimum reinforcement ratio than the minimum value given in AS3600:2009 [12]. This provision has a requirement that RC walls have a minimum ρ_{wv} of 0.15%. This minimum has been derived for the control of shrinkage and thermal effects as stated in the AS3600:2009 Commentary [18] and due considerations is not given to ductility. Furthermore, in the Earthquake Actions code of Australia AS1170.4:2007 [19] a ductility (μ) of 2 is assumed for 'limited-ductile' RC walls.

To assist in validating the SCM, an investigation has been carried out using the finite element modelling software VecTor2 [1].

4 FINITE ELEMENT MODELLING VERIFICATION

4.1 VECTOR2

VecTor2 [1] is a state-of-the-art nonlinear finite element modelling program for plane RC sections that is based on the disturbed stress field model [20]. VecTor2 has been used in a variety of past research for modelling RC walls [8, 21-26]. In order to validate the use of VecTor2, a model has been developed and compared with some experimental data. Testing has been very limited on lightly reinforced and unconfined RC walls. However, the RC wall specimen 'C1' [27] is suitable for the purposes of validating the chosen material models that will be used in VecTor2. The constitutive and material models that will be used in VecTor2 are introduced, followed by details of the C1 wall specimen. After validating VecTor2, a typical MR RC wall is introduced and modelled in VecTor2. The results of the VecTor2 analyses are then presented.

4.2 CONSTITUTIVE AND MATERIAL MODELS FOR VECTOR2

The concrete compression models used for the ensuing analyses will comply with the recommendations from [28]; for concrete strengths up to 45MPa the Popovics normal-strength concrete model will be used. For concrete strengths higher than 45MPa, which is the case for the proposed MR walls in Section 4.4, the Popovics high-strength concrete model will be used. The preliminary parameter studies conducted by [29] suggested that the compression softening model that relied only on stress, rather than both stress and strain, gave better approximations at large displacements. Therefore, Vecchio 1992-B (e1/e0-Form) [30] was chosen to model the compression softening of concrete, instead of the default Vecchio 1992-A (e1/e2-Form) [30]. The Modified Bentz model (default) is used for modelling of tension stiffening in the concrete. This is essentially the same as the Bentz 1999 [31] model for when 'the steel is aligned with the x or y-axis (no skew steel)' [32], which is used in the Modified Compression Field Theory (MCFT) for programs such as Response-2000 [33]. Of the numerous bilinear models that are proposed by different researchers for the prediction of tension softening, the CEB-FIP [34] model is utilised by VecTor2 in providing a bilinear model for the stress-strain relationship of concrete. Importantly, the default concrete fracture energy value of 75 N/m has been used in VecTor2, which is a similar assumption by

other researchers [32]. The Palermo option for modelling the concrete hysteretic response is used in this configuration, as proposed by [35], and has also been found to be a more adequate and effective option in capturing the behaviour and stiffness in other studies [36]. The dilation model chosen for the lateral expansion of concrete is the 'Variable – Orthotropic' (default), which is based on a Poisson's ratio that increases nonlinearly as the concrete compressive strain increases. The cracking criterion models estimate the decrease of cracking strength due to the increase of the transversely acting compressive stresses. The CEB-FIP Model is chosen specifically for this, which is based on a linear relationship proposed by [37]. The compressive stresses of concrete elements close to cracks are required to be limited, mainly due to tensile strains in concrete close to cracks exceeding the calibration range of compression softening models, which may permit additional softening. It can also cause problems if a shear-slip model has not been considered, which in this case it has. The crack width check ultimately reduces the average compressive stresses for when the crack width exceeds a set limit. The default was chosen ('Agg/2.5 Max Crack Width') as the limiting crack width. VecTor2 accounts for the strains due to shear slip along cracks with the element slip distortion models. The default model from [38] was chosen for these calculations. The reinforcing steel is represented by the stress-strain curve suggested by [39]. Although neglecting the strength enhancement due to confinement appears to be a viable option for unconfined RC walls investigated here, recent investigations by the authors using VecTor2 have shown that the Kupfer/Richart [40, 41] model gives overall better results for walls that are governed by compression. Bond-slip was only considered for VecTor2 models that use truss and link elements to model the longitudinal reinforcement. Otherwise, the assumption was that the reinforcement had perfect bond to the concrete, an approach that has also been adopted by [27]. Other studies have shown that the assumption of perfect bonding between the reinforcement and concrete have provided satisfactory results [28]. More details of the chosen material models can be found in [1].

4.3 C1 WALL SPECIMEN

Researchers [27, 42] reported on an experimental program in order to evaluate the seismic performance of RC walls with minimum longitudinal reinforcement in accordance with NZS 3101:2006 [43]. The wall specimen C1, shown in Figure 4.1, was designed to represent a 50% scale of a multi-story flexure-dominat RC wall with limited ductility [27] and was tested under reverse cyclic conditions. Three different methods of modelling the longitudinal reinforcement in VecTor2 were undertaken; Model 1 uses smeared reinforcement, Model 2 uses discrete truss elements and Model 3 uses discrete truss elements with link elements. The link elements act as spring elements in between the rectangular concrete elements and truss elements to model the bond-slip. The strain distribution at 1.5% drift (top wall displacement of 42mm) was also reported by [27], which will be compared to the VecTor2 results at the same lateral drift in attempting to validate the VecTor2 program for lightly reinforced walls.

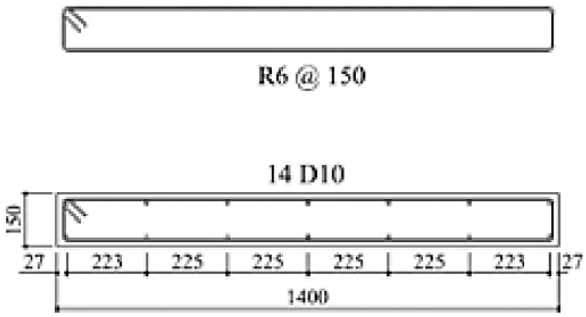

Figure 4.1: *Cross section of wall specimen C1 [27]*

Figure 4.2 illustrates the mesh and element setup of the Model 1, which represents the setup from [27] and [42]. Table 4.1 gives the number of elements and nodes used in the three different model setups. The extra nodes and/or elements for Model 2 and Model 3 are due to the truss and link elements. The foundation block at the base was assumed to be 500mm x 1820mm (x 350mm high). The concrete compressive strength was 38.5MPa, while the tensile strength of the concrete was 2.88MPa. The yield and ultimate stress of the longitudinal reinforcing 10mm diameter bars were f_y=300MPa and f_u=409MPa respectively. The ultimate strain (ε_{su}) of the longitudinal bars was found to be 153 mm/m from material testing. [44] explains that using the ε_{su} found from monontonic testing is inappropriate for moment-cruvature analysis, which could be further extrapolated as being inapproriate for assessment purposes. Therefore, $0.6\varepsilon_{su}$ will be used as suggested by [44], where the final steel strain value used is 91.8mm/m. The horizontal reinforcement is modelled with smeared reinforcement for all three models. Model 3, which utilises the link elements, use the Eligehausen [45] concrete bond model to ultimately observe the predicted amount of strain penetration into the foundation. Moreover, the bond properties for the link elements were set to 'Embedded Deformed Rebars' with a Confinement Pressure Factor of zero, corresponding to an unconfined case. Models 1 and 2 (smeared and truss) assume perfect bond. An axial load of 294kN (ALR=3.5%) was applied to all nodes at the top of the wall (held constant throughout the analysis), while the same nodes were subjected to a lateral displacement for both the monotonic or reverse cyclic loading scenarios.

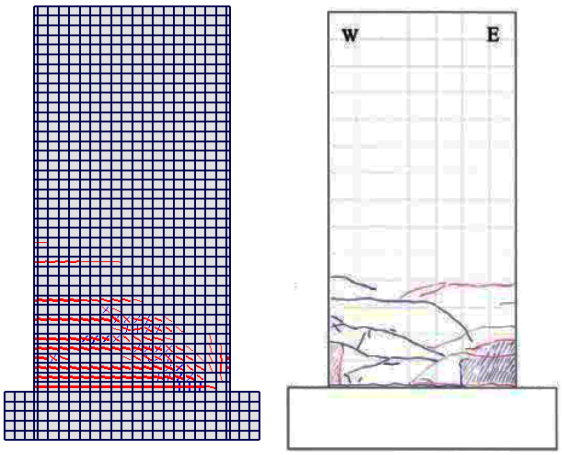

Figure 4.2: *Mesh setup and cracking distribution from VecTor2 (left) and experimental observations from [27] (right)*

Table 4.1: *Number of elements and nodes for each model used in VecTor2 for wall C1*

Model	Elements	Nodes
1	930	1002
2	1224	1002
3	1875	1646

Figure 4.3 shows the results from VecTor2 for both monotonic and reverse cyclic conditions for Model 1 (smeared). Superimposed in these figures are the experimental results from [27]. The results from VecTor2 produce a good correlation with the force-displacement hysteresis observed experimentally. The force-displacement hysteresis results for Models 2 and 3 also correlated well and are not shown here due to space limitations.

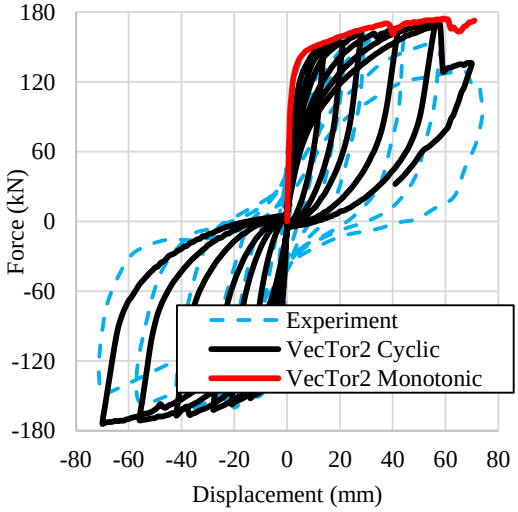

Figure 4.3: *Force-displacement results from VecTor2 for wall C1 specimen from [27]*

Figure 4.4 presents the strain distribution results in the steel from VecTor2 at the extreme fibre edge of the wall in tension for Model 1 (smeared). Superimposed in this figure are the strain distributions recorded by [27]. The strain distributions predcicted by VecTor2 correlate well with the epxeirmental observations. Furthermore, the strains predicted with cyclic loading did not differ much from the predictions with the wall subjected to monotonic loading, which was also observed by [46].

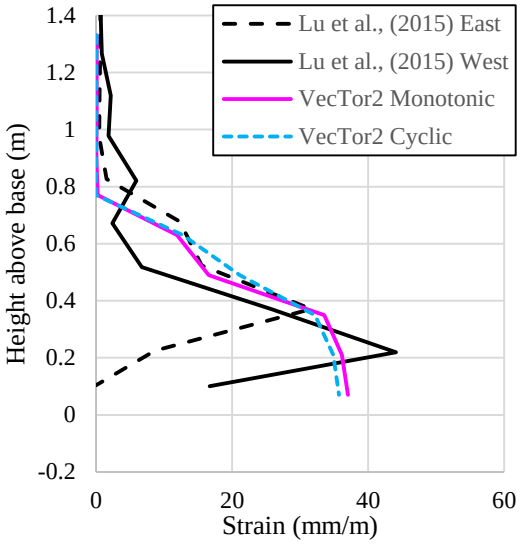

Figure 4.4: *Steel strain distribution comparison for Model 1 (smeared) at a wall drift of 1.5% (42mm top displacement)*

Figure 4.5 gives the same strain distribution results for Models 2 and 3 (truss and truss-link respectively). Both models predict a similar steel strain distribution up the wall height at the extreme fibre tension edge of the wall. The VecTor2 results over predict the steel strains higher up the wall in comparison to the experimental observations from [27] and, importantly, compared with Model 1 (smeared) shown in Figure 4.4. Model 3 (truss-link), which uses the Eligehausen [45] bond model, predicts a slightly higher steel strain into the foundation in comparison to Model 2 (truss). However, the strains predicted by both Model 2 and Model 3 are insignificant in comparison to the strains predicted above the base (0.058mm/m and 0.504mm/m respectively at a top displacement of 42mm). Furthermore, the strains predicted by Model 3 with the truss-link elements into the foundation did not reach yield (ε_{sy}≈2.00mm/m) throughout the analysis (1.28mm/m at a top displacement of 70mm).

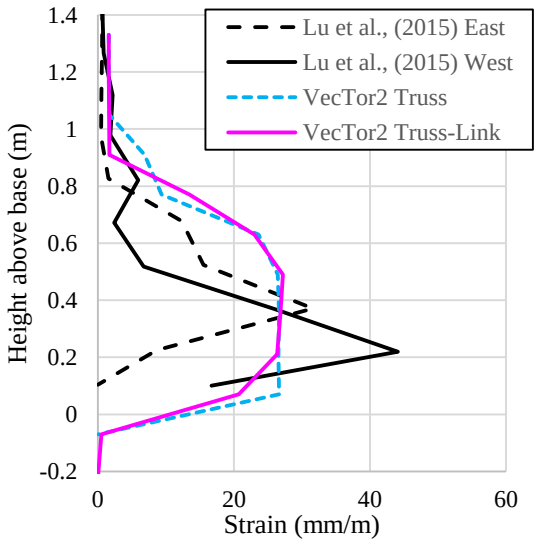

Figure 4.5: *Steel strain distribution comparison for Model 2 and 3 (truss and truss-link respectively) at a wall drift of 1.5% (42mm top displacement)*

Overall, VecTor2 has been shown to provide well correlated results to the experimental observations. Importantly, the strain distributions up the wall height are very well correlated, particularly for Model 1 (smeared). It is the strain distributions (and correspondingly, the curvature distributions) that will be used in the calculations for the equivalent plastic hinge length.

4.4 MID-RISE RC WALL

To further validate the SCM discussed in Section 3, a Mid-Rise (MR) RC rectangular wall will be modelled in VecTor2. Secondary cracking will be investigated from the results by using a range of longitudinal reinforcement ratios and typical parameters for the RC wall that would be found in low-to-moderate seismic regions, such as Australia. The proposed MR RC wall complies with the definition of MR from [47], in which 5-storeys is used. Assuming an inter-storey height of 3.5m, the total height (H_n) of the wall is 17.5m. This gives an effective height (H_e) of $0.7H_n$=12.25m, using the recommendations from [44]. The average material properties for D500N reinforcing steel will be used for the assumed 12mm diameter longitudinal and transverse reinforcement [17]. The recommendations from [44] to use $0.6\varepsilon_{su}$ as previously discussed in Section 4.3 will be used in the analyses. A f_{cmi} of 60MPa will be assumed for the reasons previous discussed in Section 3, with a $f'_{ct.f}$ of 6.07MPa. The wall is assumed to be 200mm thick (t) and 5000mm long (L_w). The recommendations from [28] to use 14-16 elements across (in the direction of the L_w) seemed to be more applicable for modelling experimental walls, which typically have smaller wall lengths due to scaling. Therefore, it was decided to have an element size within $0.5t$ to $1.0t$, which will create a much finer mesh. The recommendations by [1] to have rectangular elements within a 3:2 aspect ratio was also obeyed for the refined mesh of the bottom half of the wall (in the region of interest). The top half of the wall had elements with an increased vertical size to decrease computational time, which has also been carried out by other researchers [22]. The size of the elements in the bottom half of the wall were 125mmx125mm, while the top elements were 125mmx250mm. Based on the results from Section 4.3, the longitudinal reinforcement will be modelled as smeared and thus perfect bond will be assumed. Furthermore, the results of the C1 wall indicated that the foundation is unnecessary for the purposes of plastic hinge analysis. This is for several reasons: firstly, the strains into the foundation were negligible, as has been found from other researchers [46]. 'As yielding did not proceed into the foundation, strain penetration was concluded to be negligible and hence not included in L_p' [46]. This was also observed experimentally as shown in Figure 4.4 and Figure 4.5, where the strains appear to decrease to zero at a height above the foundation. Secondly, the smeared reinforcement model (Model 1) yielded higher correlated results to the experimental observations in comparison to the truss element models (Figure 4.4 compared to Figure 4.5). Thirdly, other researchers have neglected the foundation when investigating the plastic hinge length of RC walls [22]. Using smeared reinforcement and neglecting the foundation will also be less computationally expensive. Smeared reinforcement was also used for the transverse reinforcement throughout the concrete material assigned to the 3000 elements (3116 nodes). The longitudinal reinforcement ratio (ρ_{wv}) was varied between 0.19 to 1.2%, where RC walls with ρ_{wv} less than 1% are considered to 'represent the great majority of building stock in low-to-moderate seismic regions such as Australia' [2]. Two layers of reinforcement are assumed to be used throughout the wall length and height (longitudinal and transverse). An exception to this was the wall with 0.19% ρ_{wv}, which only had one layer. The spacing (s) minimum and maximum of the reinforcement from AS3600:2009 was obeyed, which corresponded to using d_{bl} of 12mm and 16mm. An axial load ratio (ALR) of 5% was used, where ALRs of less than 5% are common in walls with low vertical reinforcement [6]. Moreover, the RC walls investigated by [48] for low-to-moderate seismic regions indicated that most of the walls had ALRs less than 5%, and the highest ALR did not exceed 10%. This corresponded to an axial load of 3000kN, which was held constant throughout the analyses. The lateral loading was monotonically increased at the top of the wall (H_e), controlled by displacement, until failure. 'Failure' of the wall was deemed to occur with the strain limits offered by [49] for the collapse prevention limit state for

unconfined RC walls in low-to-moderate seismic regions; that is an ultimate strain of steel (ε_{su}) and concrete (ε_{cu}) of 15mm/m and 3mm/m respectively.

4.5 VECTOR2 RESULTS

The cracking distributions for the MR wall with ρ_{wv} of 0.80%, 1.00%, 1.20% and 1.30% is shown in Figure 4.6. It is evident from Figure 4.6 that the onset of secondary cracking, between primary cracks, occurs for the MR wall with a ρ_{wv} of approximately 1.20%. The majority of the analyses conducted in VecTor2 for the MR with a range of ρ_{wv} failed in flexure with the tension strains governing. However, the two walls with ρ_{wv} of 1.30% and 1.40% failed in compression (reaching a ε_{cu} of 3mm/m).

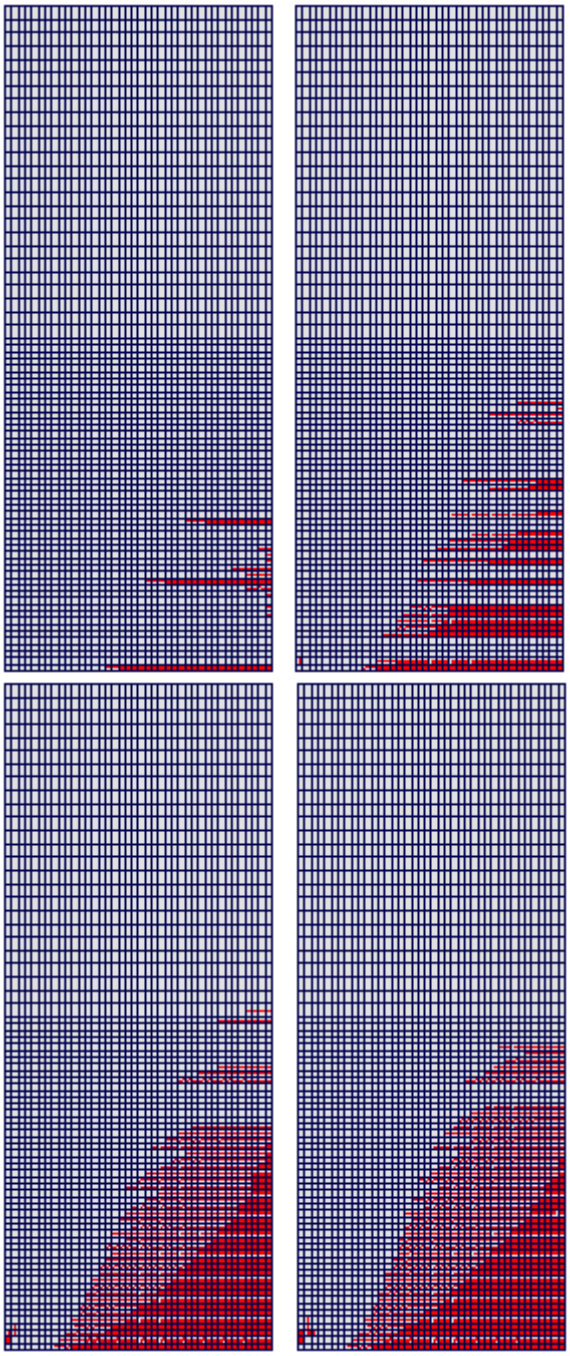

Figure 4.6: *Cracking distributions at collapse prevention limit state for the MR with ρ_{wv} of 0.80% (top left), 1.00% (top right), 1.20% (bottom left) and 1.30% (bottom right)*

To further illustrate the onset of secondary cracking using the VecTor2 results, the equivalent plastic hinge length is calculated for each of the walls.

5 EQUIVALENT PLASTIC HINGE LENGTH METHOD

The plastic hinge length is the distance in the critical region of the member for bending over which inelastic strains/curvatures occur. It is common practice to calculate an equivalent length or height over which the inelastic curvatures are uniform and equal to the plastic curvature, Φ_p, and this is called the equivalent plastic hinge length (L_p). An approximate method has been developed and used to calculate this "equivalent" length such that the resulting plastic rotation is representative of that in the actual wall.

This approximate method is briefly summarised here. It uses the curvatures up the height of the wall to determine the equivalent length over which inelastic curvatures are occurring from the base. The distributions of curvatures can be separated into two regions, the elastic region (Equation 5) and the plastic region (Equation 6).

$$\theta_e = \frac{1}{2}\int_0^{H_e} \emptyset_y \, dx \tag{5}$$

$$\theta_p = \int_0^{L_y} \left|\emptyset(x) - \emptyset_y(x)\right| dx \tag{6}$$

The L_p can be calculated by assuming that the plastic rotation (θ_p) is equivalent to a rectangle of width Φ_p (plastic curvature) and height L_p.

$$\theta_p = \emptyset_p L_p \tag{7}$$

$$L_p = \frac{\theta_p}{\emptyset_p} = \frac{\theta_p}{\emptyset_u - \emptyset_y} \tag{8}$$

Curvature distributions of the MR walls with varying longitudinal reinforcement ratio analysed in Section 4 were obtained from Janus [50, 51], a post-processing program for VecTor2. The curvatures were calculated up the wall height by taking the steel (ε_s) and concrete (ε_c) strains at each of the respective extreme fibres (at the same height of the wall) and calculating the curvatures. The curvature distribution was calculated corresponding to when the collapse prevention strain limit was reached in either the steel or concrete, as discussed in Section 4.4. Figure 5.1 gives the results of the L_p that has been calculated using Equations 5 to 8 for the MR walls as a function of the varying ρ_{wv}. Superimposed in this figure (shaded region) is indication of the $\rho_{wv.min}$ estimated from the SCM of

0.81% and 1.21% excluding and including the axial stress respectively, discussed in Section 3. The estimation from the SCM seems to indicate the onset of the increasing L_p with increasing ρ_{wv}. The decrease in L_p for the walls with a ρ_{wv} of 1.30% and 1.40% could be explained due to these walls failing in compression rather than tension. The L_p for the walls with ρ_{wv} less than the minimum estimated from the SCM ($\rho_{wv.min}$≈0.81%) are all approximately 25mm. Interestingly, this was close to $2d_b$. Recent field observations of the RC buildings after the Christchurch earthquake [9] indicated that the effective plastic hinge length for single-crack failed walls may be restricted to the true length of the yield penetration length (L_{yp}). A lower bound of 1 to 2 times d_b is offered by [9] for L_{yp}.

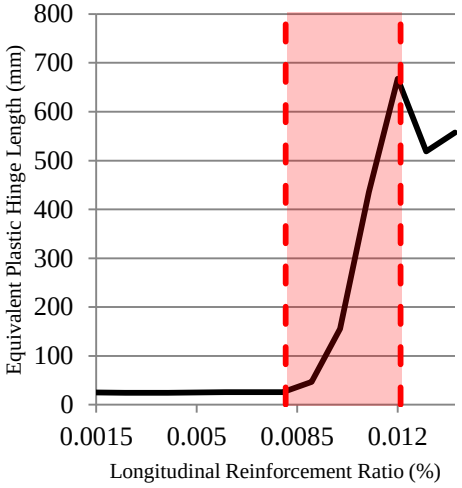

Figure 5.1: *Plastic hinge lengths for the mid-rise wall with vary longitudinal reinforcement*

Figure 5.2 gives the results of the L_p that has been calculated for the MR walls as a function of the ratio of the ultimate moment capacity of the wall (M_u) to the cracking moment (M_{cr}). It should be noted that M_u was taken at the collapse prevention limit state corresponding to the strain limits. It is clear from Figure 5.2 that a fairly sufficient moment capacity in the wall is needed for a distribution of plasticity and correspondingly for a ductile response. This is in the order of a M_u/M_{cr} of about 2.0 to 3.0, larger than the $1.2M_{cr}$ that is required for the design of bending for beams given in AS3600:2009 [12], and by implication for the design of RC walls as previously discussed in Section 3 and suggested by [13]. The arbitrary value of 1.2 doesn't appear to have any statistical basis, where others such as [52] have recommended a nominal moment capacity of a concrete section with minimum reinforcement to be at least $1.5M_{cr}$, and [9] further suggests 1.5 to 2.0 times M_{cr} be used.

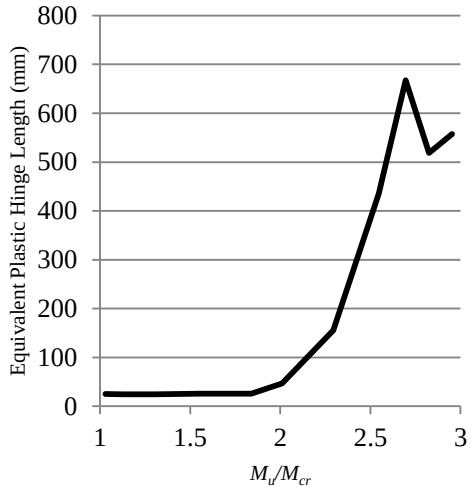

Figure 5.2: *Plastic hinge lengths for the mid-rise wall as a function of the cracking moment to ultimate moment capacity ratio*

6 CONCLUSION

The Secondary Cracking Model (SCM) was introduced, which can be used to predict the longitudinal reinforcement required to initiate secondary cracking in RC walls. VecTor2, a state-of-the-art finite element modelling program, was used to validate the SCM, showing good correlations with the equivalent plastic hinge lengths (L_p) and the estimation of $\rho_{wv.min}$. The L_p was also shown as a function of M_u/M_{cr}, which illustrated that a wall needs to have a considerably higher moment capacity than the cracking moment in order to achieve a distribution of plasticity. Further analyses are being conducted at the University of Melbourne to ultimately derive a plastic hinge length which can be used to aid in estimating the displacement capacity of lightly reinforced walls.

ACKNOWLEDGEMENT

The support of the Commonwealth of Australia through the Bushfire and Natural Hazards Cooperative Research Centre program is acknowledged.

REFERENCES

1. Wong, P. and F. Vecchio, *Vector2 and FormWorks User Manual. Department of Civil Engineering, University of Toronto*. 2002.
2. Wibowo, A., et al. *Seismic performance of lightly reinforced structural walls for design purposes*. Magazine of Concrete Research, 2013. 65, 809-828.
3. Wilson, J., et al., *Drift behaviour of lightly reinforced concrete columns and structural walls for seismic design*

applications. Australian Journal of Structural Engineering, 2015. 16(1): p. 62-74.
4. CERC, C.E.R.C., *Final report: Volume 2: The performance of Christchurch CBD Buildings*. 2012: Wellington, NZ.
5. Wood, S., R. Stark, and S. Greer, *Collapse of Eight-Story RC Building during 1985 Chile Earthquake.* Journal of Structural Engineering, 1991. 117(2): p. 600-619.
6. Henry, R.S., *Assessment of the Minimum Vertical Reinforcement Limits for RC Walls.* Bulletin of the New Zealand Society for Earthquake Engineering, 2013. 46(2): p. 88.
7. Henry, R.S., J. Ingham, and Y. Lu, *Experimental testing and modelling to address the performance of RC walls during the 2010/2011 Canterbury earthquakes*, in *Tenth U.S. National Conference on Earthquake Engineering*. 2014: Anchorage, Alaska.
8. Sritharan, S., et al., *Understanding Poor Seismic Performance of Concrete Walls and Design Implications.* Earthquake Spectra, 2014. 30(1): p. 307-334.
9. Morris, G.J., D.K. Bull, and B.A. Bradley, *In Situ Conditions Affecting the Ductility Capacity of Lightly Reinforced Concrete Wall Structures in the Canterbury Earthquake Sequence.* Bulletin of the NZ Society of Earthquake Engineering, 2015. 48(3): p. 191-204.
10. Goldsworthy, H.M. and G. Gibson. *Changes in Seismic Design Philosophy for RC Structures in Areas of Low to Moderate Seismicity Following the Christchurch Earthquake*. in *15th World Conference in Earthquake Engineering*. 2012. Lisbon, Portugal.
11. Patel, V.J., et al., *Effect of reinforcing steel bond on the cracking behaviour of lightly reinforced concrete members.* Construction and Building Materials, 2015. 96: p. 238-247.
12. Standards Australia, *AS 3600-2009: Concrete Structures.* 2009.
13. Beletich, A.S., et al., *Reinforced concrete : the designers handbook*. 2013: Baulkham Hills, N.S.W. Cement and Concrete Services, 2013.
14. fib, F.I.d.B., *Model Code 2010 - Final draft, Volume 2. fib Bulletin No. 66*. 2012, Lausanne, Switzerland.
15. Hyland, *Pyne Gould Corportation Building Site Examination and Materials Tests*. 2011, Report prepared for: Department of Building and Housing.
16. Smith, P. and V. England, *Independent Assessment on Earthquake Performance of Gallery Apartments - 62 Gloucester Street*. 2012, Report prepared for the Canterbury Earthquakes Royal Commision, available at http://canterbury.royalcommission.govt.nz/documents-by-key/20120217.3188.
17. Menegon, S.J., H.H. Tsang, and J.L. Wilson. *Overstrength and ductility of limited ductile RC walls: from the design engineers perspective*. in *Proceedings of the Tenth Pacific Conference on Earthquake Engineering*. 2015. Sydney, Australia.
18. Standards Australia, *AS 3600-2009 Supp 1:2014 : Concrete structures - Commentary (Supplement to AS 3600-2009).* 2014.
19. Standards Australia, *AS 1170.4-2007: Structural design actions, Part 4: Earthquake actions in Australia.* 2007.
20. Vecchio, F., et al., *Disturbed Stress Field Model for Reinforced Concrete: Validation.* Journal of Structural Engineering, 2000. 126(9): p. 1070.
21. Beyer, K., *Seismic design of torsionally eccentric buildings with U-shaped RC Walls*, in *European School for Advanced Studies in Reduction of Seismic Risk*. 2007, ROSE School.
22. Bohl, A. and P. Adebar, *Plastic Hinge Lengths in High-Rise Concrete Shear Walls.* ACI Structural Journal, 2011. 108(2): p. 148-157.
23. Dai, H., *An Investigation of Ductile Design of Slender Concrete Structural Walls*. 2011, Iowa State University: Ames, Iowa.
24. Ghorbani-Renani, I., et al., *Modeling and Testing Influence of Scaling Effects on Inelastic Response of Shear Walls.* Structural Journal, 2009. 106(3).
25. Lu, Y., R.S. Henry, and Q. Ma, *Modelling and Experimental Plan of Reinforced Concrete Walls with Minimum Vertical Reinforcement*, in *Tenth U.S. National Conference on Earthquake Engineering*. 2014: Anchorage, Alaska.
26. Luu, H., P. Léger, and R. Tremblay, *Seismic demand of moderately ductile reinforced concrete shear walls subjected to high-frequency ground motions.* Canadian Journal of Civil Engineering, 2013. 41(2): p. 125-135.
27. Lu, Y., et al., *Experimental testing and modelling of reinforced concrete walls with minimum vertical reinforcement*, in *2015 New Zealand Society for Earthquake Engineering Annual Technical Conference*. 2015: Rotorua, New Zealand.

28. Palermo, D. and F.J. Vecchio, *Simulation of Cyclically Loaded Concrete Structures Based on the Finite-Element Method.* Journal of Structural Engineering, 2007. 133(5): p. 728-738.
29. Mohr, D.S., *Nonlinear Analysis and Performance Based Design Methods for Reinforced Concrete Coupled Shear Walls*, in *Department of Civil and Environmental Engineering*. 2007, University of Washington: Seattle, U.S.A.
30. Vecchio, F., *Finite Element Modeling of Concrete Expansion and Confinement.* Journal of Structural Engineering, 1992. 118(9): p. 2390-2406.
31. Bentz, E.C., *Sectional Analysis of Reinforced Concrete Structures*, in *Department of Civil Engineering*. 1999, University of Toronto: Toronto, Ontario.
32. Bohl, A., *Plastic Hinge Length in High-Rise Concrete Shear Walls*, in *The Faculty of Graduate Studies - Civil Engineering*. 2003, The University of British Columbia.
33. Bentz, E.C., *RESPONSE-2000: Sectional Analysis of Reinforced Concrete Members*. 2000: University of Toronto.
34. CEB-FIP, C.E.-I.d.B., *CEB-FIP Model Code 1990*. 1990, Thomas Telford: London.
35. Palermo, D. and F. Vecchio, *Behaviour and Analysis of Reinforced Concrete Walls Subjected to Reversed Cyclic Loading.* Publication No. 2002-01, Department of Civil Engineering, University of Toronto, 351 pp., 2002.
36. Sagbas, G., *Nonlinear Finite Element Analysis of Beam-Column Subassemblies*, in *Graduate Department of Civil Engineering*. 2007, University of Toronto: Toronto, Canada.
37. Kupfer, H.B. and K.H. Gerstle, *Behavior of Concrete under Biaxial Stresses.* Journal of the Engineering Mechanics Division, 1973. 99(4): p. 13.
38. Walraven, J.C., *Fundamental Analysis of Aggregate Interlock.* Journal of the Structural Division, 1981. 107(11): p. 25.
39. Seckin, M., *Hysteretic Behaviour of Cast-in-Place Exterior Beam-Column-Slab Subassemblies*, in *Department of Civil Engineering*. 1981, University of Toronto: Toronto, Canada. p. 266.
40. Kupfer, H., H.K. Hilsdorf, and H. Rusch, *Behavior of Concrete Under Biaxial Stresses.* Journal Proceedings, 1969. 66(8).
41. Richart, F.E., A. Brandtzaeg, and R.L. Brown, *A study of the failure of concrete under combined compressive stresses.* University of Illinois Bulletin; v. 26, no. 12, 1928.
42. Henry, R.S., et al. *Recent Research to Improve the Seismic Performance of Lightly Reinforced and Precast Concrete Walls*. in *Proceedings of the Tenth Pacific Conference on Earthquake Engineering*. 2015. Sydney, Australia.
43. Standards Association NZ, *NZS 3101: Part1:2006, "Concrete Structures Standard - The Design of Concrete Structures"*. 2006.
44. Priestley, M.J.N., G.M. Calvi, and M.J. Kowalsky, *Displacement-based seismic design of structures / M. J. N. Priestley, Gian Michele Calvi, Mervyn J. Kowalsky*. 2007: Pavia : IUSS Press : Fondazione Eucentre, 2007.
45. Eligehausen, R., *Local bond stress-slip relationships of deformed bars under generalized excitations : experimental results and analytical model*, E.P. Popov and V.V. Bertero, Editors. 1983, Earthquake Engineering Research Center, College of Engineering, University of California :: Berkeley, Calif. :.
46. Hannewald, P., *Seismic Behavior of Poorly Detailed RC Bridge Piers*. 2013, EPFL.
47. FEMA, *HAZUS MH MR5 Technical Manual*. 2010: Washington, D.C.
48. Albidah, A., et al. *A Reconnaissance Survey on Shear Wall Characteristics in Regions of Low-to-Moderate Seismicity*. in *Paper presented at the Australian Earthquake Engineering Society 2013 Conference*. 2013. Hobart, VIC.
49. Hoult, R.D., H.M. Goldsworthy, and E. Lumantarna. *Improvements and difficulties associated with the seismic assessment of infrastructure in Australia*. in *Australasian Fire and Emergency Service Authorities Council (AFAC) 2015 conference*. 2015. Adelaide, South Australia.
50. Chak, I.N., *Janus: A Post-Processor for VecTor Analysis Software*, in *Graduate Department of Civil Engineering*. 2013, University of Toronto: Toronto, Canada.
51. Jodai, A., *Nonlinear Finite Element Analysis and Post-Processing of Reinforced Concrete Structures under Transient Creep Strain*, in *Graduate Department of Civil Engineering*. 2013, University of Toronto: Toronto, Canada.
52. Paulay, T. and M.J.N. Priestley, *Seismic design of reinforced concrete and masonry buildings / T. Paulay, M.J.N. Priestley*. 1992: New York : Wiley, c1992.